Effects of Interface Bonding on Acoustic Wave Generation in an Elastic Body by Surface-Mounted Piezoelectric Transducers

Peng Li, Feng Jin, Weiqiu Chen, and Jiashi Yang

***Abstract*—We study the effects of interface bonding on acoustic wave generation in an elastic body using surface-mounted piezoelectric transducers driven electrically. A theoretical analysis is performed based on a physical model of a piezoelectric layer on an elastic substrate. The transducer–substrate interface is described by the shear-slip model, representing a viscoelastic interface. Different from the results in the literature on free vibrations of structures with weak interfaces, this paper presents an electrically forced vibration analysis. An analytical solution for the generated acoustic wave is obtained and used to calculate its energy flux and the efficiency of the transduction. The effects of the interface parameters are examined. It is found that the interface bonding affects the performance of the transducer in multiple ways, some of which may be exploitable in designs for better transducer performance. In particular, optimal transduction is not necessarily associated with a perfectly bonded interface.**

I. Introduction

Multilayered plates with interfaces among layers of different materials are common structures in many engineering fields. Very often a gluing substance, e.g., epoxy, is applied to the interfaces. Alternatively, the molecules of the neighboring materials may interpenetrate into each other to form a bonding layer. Ideally, in the simplest mechanics description, an interface is treated as a geometric surface where perfect or rigid bonding with continuous displacement and traction is assumed. In reality, an interface may be viewed physically as a thin layer with its own material properties. People have developed interface models with different levels of sophistication. Interface properties and their effects have been studied experimentally [1]–[4] and theoretically for both static and dynamic problems [5]–[8]. Specifically, for time-harmonic motions relevant to the present paper, wave propagation in unbounded domains [9]–[21] and vibrations of finite bodies [22]–[26] have been analyzed for various applications including material characterization, structural strength consideration, acoustic wave sensors, and nondestructive evaluation. These are mostly free vibration analyses regarding wave speed or frequency. More references can be found in a review article [27]. Examination of the literature shows the lack of electrically forced vibration analyses of transducers with weak interfaces. A forced vibration analysis is necessary to obtain transducer admittance and efficiency, which are fundamental transducer characteristics.

The present paper is concerned with the effects of interface bonding on acoustic wave generation in an elastic body with surface-bonded piezoelectric transducers driven electrically. In conventional analyses of this type of problem, perfect bonding between the piezoelectric transducer and the elastic body is routinely assumed. The effects of the viscoelasticity of epoxy or other glues at an interface on the electrical admittance of the transduction structure, the energy flux of the acoustic wave generated, and the efficiency of the transduction have not been well studied and understood. Our theoretical analysis is based on a mechanics model of a piezoelectric layer as a transducer bonded to an elastic substrate with their interface described by the shear-slip model [6], [7] for an imperfect, weak, or nonrigid interface. This interface model allows for a discontinuity of the tangential displacements across the interface while the traction is still continuous. The interface has its own viscoelasticity but not inertia. Such a model can describe the most basic behavior of an interface and has often been used in free vibration analyses. The shear-slip model will be introduced in Section II, along with a piezoelectric–elastic structure and its governing equations. An analytical solution is obtained in Section III. Numerical results and discussions are presented in Section IV. Some conclusions are drawn in Section V.

II. Governing Equations

Consider the structure of a piezoelectric layer on an elastic half-space, shown in Fig. 1. The piezoelectric layer is ceramic poled along the x_3-direction, which is determined from x_1 and x_2 by the right-hand rule. It is electroded at its two surfaces and is driven by an alternating voltage across the electrodes. Because of the specific orientation of the poling direction of the ceramics and the direction of the applied electric field, shear-horizontal or

Manuscript received December 25, 2012; accepted June 18, 2013. This work was supported by the National Natural Science Foundation of China (numbers 11272247 and 11090333), the National 111 Project of China (number B06024), and the Scholarship Award for Excellent Doctoral Student granted by Ministry of Education. It was also supported by the US Army Research Laboratory/US Army Research Office under agreement number W911NF-10-1-0293.

P. Li and F. Jin are with the State Key Laboratory for Mechanical Structure Strength and Vibration, Xi'an Jiaotong University, Xi'an, Shaanxi, China (e-mail: jinfengzhao@263.net).

W. Chen is with the Department of Engineering Mechanics, Zhejiang University, Hangzhou, Zhejiang, China (e-mail: chenwq@zju.edu.cn).

J. Yang is with the Department of Mechanical and Materials Engineering, University of Nebraska–Lincoln, Lincoln, NE (e-mail: jyang1@unl.edu).

DOI http://dx.doi.org/10.1109/TUFFC.2013.2780

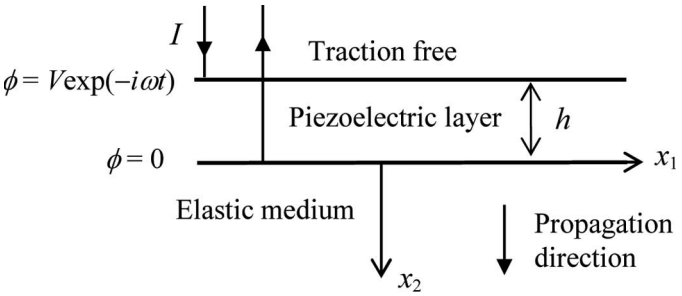

Fig. 1. A ceramic plate on an elastic half space.

antiplane waves are generated in the elastic half-space, propagating away from the ceramic plate.

For the purpose of this paper, it is sufficient to consider motions independent of x_1 and x_3. The only mechanical displacement component $u_3 = u$ and the electrical potential ϕ can be written as

$$u = u(x_2, t), \quad \phi = \phi(x_2, t). \tag{1}$$

They are governed by [28]–[30]

$$\begin{aligned} &\bar{c}\nabla^2 u = \rho\ddot{u}, \quad \nabla^2\psi = 0, \quad \phi = \psi + \frac{e}{\varepsilon}u, \quad -h < x_2 < 0, \\ &\hat{c}\nabla^2 u = \hat{\rho}\ddot{u}, \qquad\qquad\qquad\qquad\qquad\quad x_2 > 0, \end{aligned} \tag{2}$$

where ψ is a function introduced for convenience [28]–[30]. $\bar{c} = c_{44} + e_{15}^2/\varepsilon_{11}$ and ρ are the piezoelectrically stiffened shear elastic constant and the mass density of the ceramic layer. $\varepsilon = \varepsilon_{11}$ and $e = e_{15}$ are the dielectric and piezoelectric constants of the layer. $\hat{c}$ and $\hat{\rho}$ are the shear elastic constant and mass density of the elastic substrate. $\nabla^2 = \partial^2/\partial x_1^2 + \partial^2/\partial x_2^2$ is the two-dimensional Laplacian operator. The boundary and continuity conditions at the top of the piezoelectric layer and the interface between the layer and the substrate are

$$T_{23}(x_2 = -h) = 0, \tag{3a}$$

$$\phi(x_2 = -h) - \phi(x_2 = 0) = V\exp(-i\omega t), \tag{3b}$$

$$T_{23}(x_2 = 0^-) = K[u(x_2 = 0^+) - u(x_2 = 0^-)], \tag{3c}$$

$$T_{23}(x_2 = 0^+) = K[u(x_2 = 0^+) - u(x_2 = 0^-)], \tag{3d}$$

where (3c) and (3d) are based on the shear-slip model for an elastic interface. K is the effective interface elastic constant. $K = \infty$ represents a perfectly or rigidly bonded interface. When $K = 0$, the layer and the substrate lose their mechanical interaction. In harmonic motions, a complex K describes a viscoelastic interface. In addition to (3), when $x_2 \to +\infty$, the waves generated by the piezoelectric layer must be outgoing toward $+\infty$ (radiation condition).

The free charge density on the upper electrode at $x_2 = -h$ and the density of the current flowing into this electrode are given by

$$q = D_2, \quad I = \dot{q} = -i\omega q. \tag{4}$$

Then, the frequency-dependent admittance A of the structure per unit electrode area can be determined from

$$I = AV. \tag{5}$$

With the complex notation for harmonic motions, the input electrical power is given by

$$P_1 = \frac{1}{4}(IV^* + I^*V), \tag{6}$$

where an asterisk represents a complex conjugate. The instantaneous energy flux of the waves generated in the elastic medium can be calculated from

$$s_2 = -T_{23}\dot{u}, \tag{7}$$

in which real fields must be used, which are taken from the real or imaginary parts of complex fields. We denote its average over a period by $P_2 = -(T_{23}\dot{u}^* + T_{23}^*\dot{u})/4$. Then, the efficiency for the acoustic wave generation by the applied electric field is calculated from

$$\eta = P_2/P_1. \tag{8}$$

III. Forced Vibration Solution

For $-h < x_2 < 0$, the solution can be written as

$$\begin{aligned} u &= (A_1\cos\xi x_2 + A_2\sin\xi x_2)\exp(-i\omega t), \\ \psi &= (B_1 x_2 + B_2)\exp(-i\omega t), \end{aligned} \tag{9}$$

where A_1, A_2, B_1, and B_2 are undetermined constants, and

$$\xi^2 = \frac{\rho\omega^2}{\bar{c}}. \tag{10}$$

The relevant stress component and the electric potential needed for the boundary conditions can be obtained from (9) as

$$\begin{aligned} T_{23} &= \bar{c}u_{,2} + e\psi_{,2} \\ &= (-\bar{c}A_1\xi\sin\xi x_2 + \bar{c}A_2\xi\cos\xi x_2 + eB_1)\exp(-i\omega t), \\ \phi &= \psi + \frac{e}{\varepsilon}u \\ &= \left(\frac{e}{\varepsilon}A_1\cos\xi x_2 + \frac{e}{\varepsilon}A_2\sin\xi x_2 + B_1 x_2 + B_2\right)\exp(-i\omega t). \end{aligned} \tag{11}$$

For $x_2 > 0$, the solution can be written as

$$u = \hat{A}\exp i(\hat{\xi}x_2 - \omega t), \tag{12}$$

where $\hat{A}$ is an undetermined constant, and

$$\hat{\xi}^2 = \frac{\hat{\rho}\omega^2}{\hat{c}}. \tag{13}$$

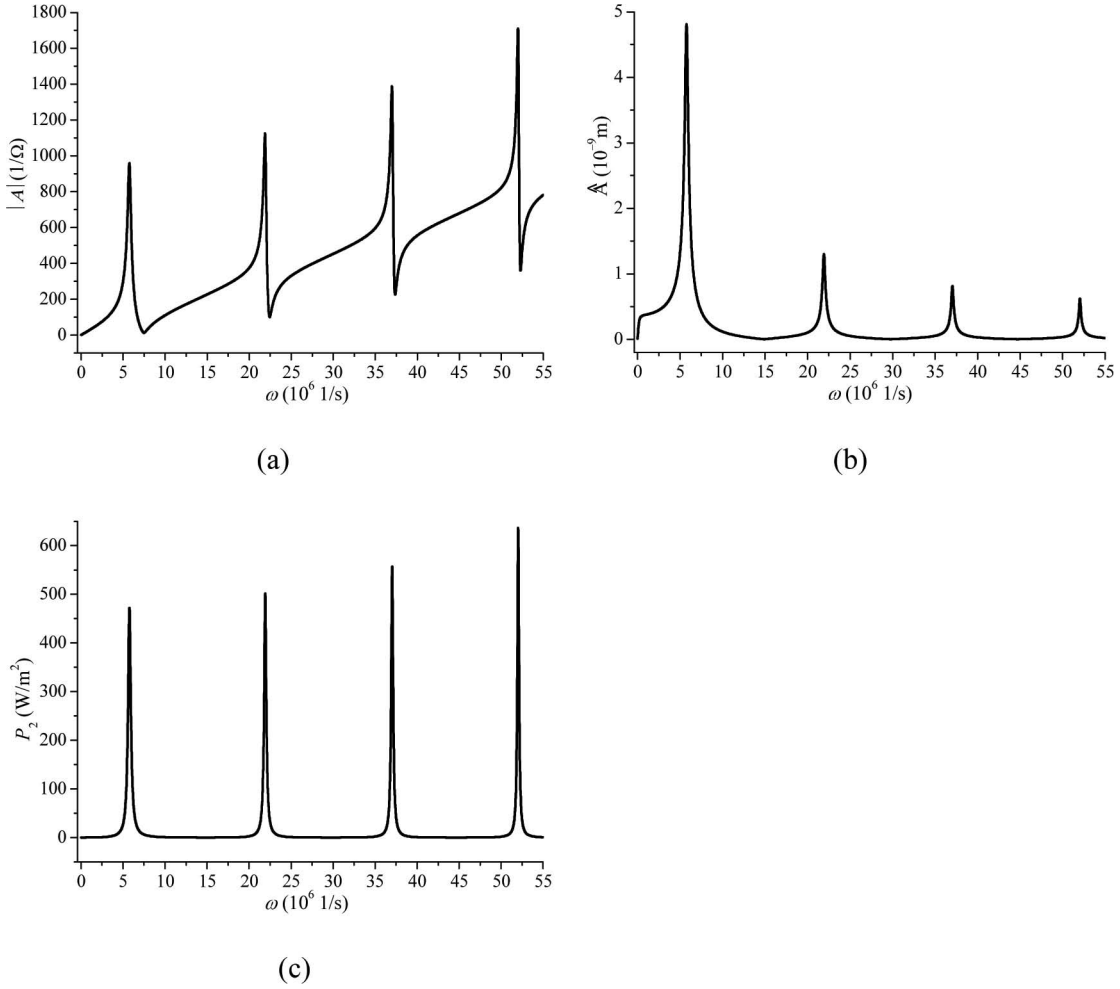

Fig. 2. The first few resonances of (a) admittance $|A|$; (b) amplitude $|\hat{A}|$ of the generated wave; and (c) energy flux P_2 of the generated wave ($K_0 = 1 \times 10^{14}$ N/m^3 and $K_1 = 0.1K_0$).

We note that (12) represents waves propagating in the positive direction of the x_2-axis, which already satisfies the radiation condition. For interface continuity conditions, we need

$$T_{23} = \hat{c}u_{,2} = \hat{c}i\hat{\xi}\hat{A}\exp i(\hat{\xi}x_2 - \omega t). \tag{14}$$

Substituting (9), (11), (12), and (14) into (3) results in the following four linear algebraic equations for A_1, A_2, B_1, and $\hat{A}$, driven by V:

$$\begin{aligned}
&\overline{c}A_1\xi\sin\xi h + \overline{c}A_2\xi\cos\xi h + eB_1 = 0,\\
&\frac{e}{\varepsilon}A_1\cos\xi h - \frac{e}{\varepsilon}A_2\sin\xi h - B_1 h + B_2 - \frac{e}{\varepsilon}A_1 - B_2 = V,\\
&\overline{c}A_2\xi + eB_1 = K(\hat{A} - A_1),\\
&\hat{c}i\hat{\xi}\hat{A} = K(\hat{A} - A_1).
\end{aligned} \tag{15}$$

Solving (15), we obtain the amplitude of the generated wave in the substrate as

$$\hat{A} = \frac{e}{\overline{c}}\frac{1-\cos\xi h}{\Delta}V = \frac{e}{\overline{c}}\frac{1-\cos\xi h}{\Delta_1 + \Delta_2}V, \tag{16}$$

where

$$\begin{aligned}
\Delta_1 &= (1-\cos\xi h)\left[k^2(\cos\xi h - 1) - i\frac{\hat{c}}{\overline{c}}\hat{\xi}h\right]\\
&\quad + \left(\sin\xi h + i\frac{\hat{c}\hat{\xi}}{\overline{c}\xi}\right)(\xi h - k^2\sin\xi h),\\
\Delta_2 &= \frac{i\hat{c}\hat{\xi}}{K}[k^2(2-2\cos\xi h) - \xi h\sin\xi h],
\end{aligned} \tag{17}$$

in which $k^2 = e^2/(\varepsilon\overline{c})$ is the shear electromechanical coupling coefficient of the piezoelectric material. $\Delta = 0$ yields the frequency equation for free vibration.

IV. Numerical Results and Discussion

As a numerical example, consider a ceramic plate of PZT-5H with $c = 2.3 \times 10^{10}$ N/m^2, $e = 17$ C/m^2, $\varepsilon =$

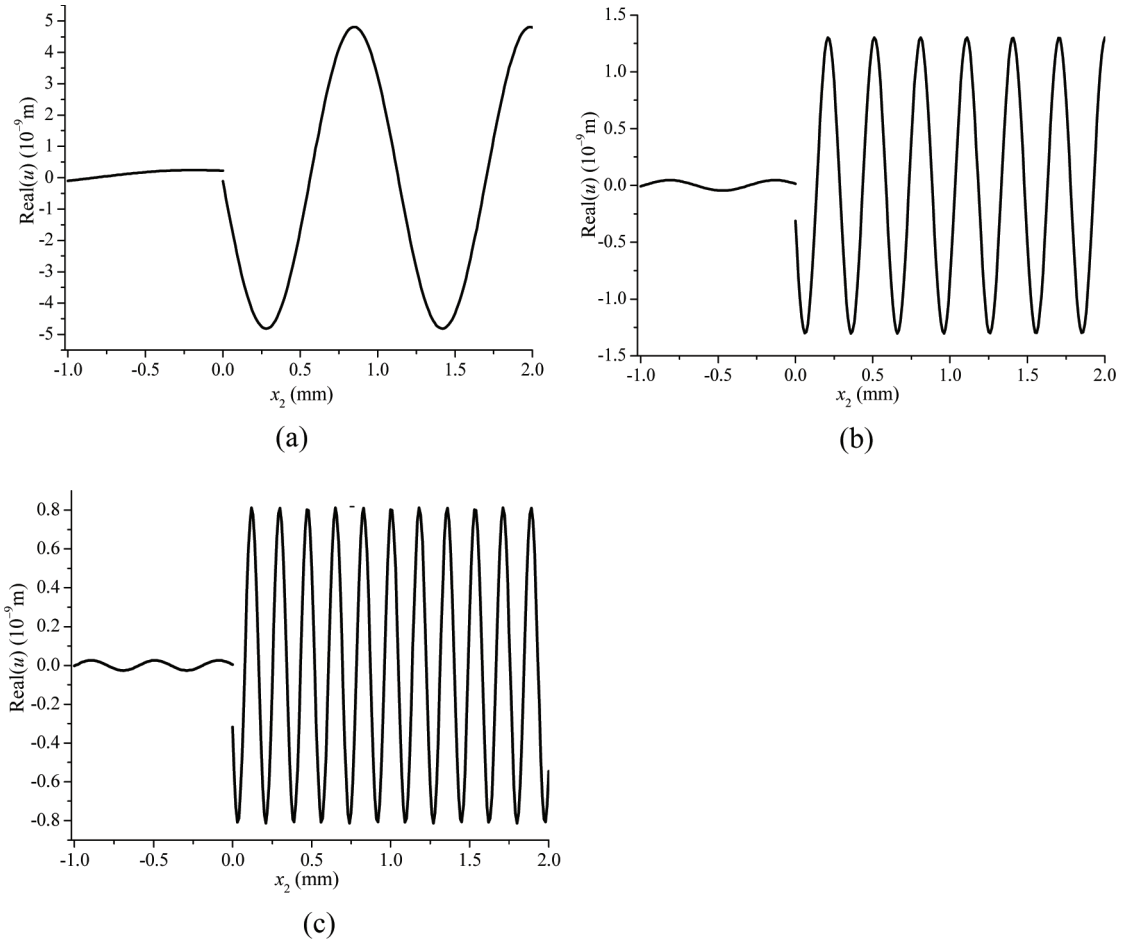

Fig. 3. Displacement distribution along x_2 at the first three resonances.

1.506×10^{-8} F/m, and $\rho = 7500$ kg/m^3. For the substrate, we consider polythene [31] with $\hat{c} = 0.128 \times 10^{10}$ N/m^2 and $\hat{\rho} = 1180$ kg/m^3. $h = 1$ mm and $V = 1$ V are used. In this case, the substrate is more compliant and lighter than the transducer material. Because the interface glue is usually viscoelastic, we use a complex interface stiffness whose imaginary part describes interface damping. Let $K = K_0 - iK_1$, where both K_0 and K_1 are real and positive. A negative imaginary part is used to be consistent with the $\exp(-i\omega t)$ factor in our complex notation. We begin with $K_0 = 1 \times 10^{14}$ N/m^3 and $K_1 = 0.1K_0$, which will be varied later. $K_1 = 0.1K_0$ represents relatively large damping, which is chosen to more clearly show the resonances graphically.

Figs. 2(a), 2(b), and 2(c) show the admittance $|A|$ per unit area, the amplitude $|\hat{A}|$ of the generated wave, and the energy flux P_2 of the generated wave versus the driving frequency, respectively. The frequencies at which the admittance assumes maxima are the resonant frequencies. At resonances, the amplitude and the output energy flux also assume maxima. At these frequencies, significant acoustic wave generation can be realized.

When $K_0 = 1 \times 10^{14}$ N/m^3 and $K_1 = 0.1K_0$, corresponding to the first three resonances in Fig. 2, the distribution of the displacement u along x_2 is shown in Fig. 3. At the interface between the plate and the substrate, the displacement is discontinuous, as described by the shear-slip model. This discontinuity is larger for higher-order modes. For higher-order modes, there are more nodal points (zeros) along the plate thickness. The wavelength becomes shorter in both the plate and the substrate for higher-order modes. In the example shown, the amplitude in the substrate is significantly larger than that in the plate, whereas the energy flux in Fig. 2(c) does not change much for different modes.

The effects of the interface stiffness K_0 on the admittance $|A|$, the amplitude $|\hat{A}|$ of the generated wave, and the energy flux P_2 of the generated wave near the first resonance locally are shown in Fig. 4, where $K_1 = 2 \times 10^{13}$ N/m^3. The resonant frequency is sensitive to the interface stiffness, as expected. When K_0 decreases, the resonant frequency decreases because there is less stiffness in the structure. It is interesting and potentially useful to see that when the interface bonding becomes weaker, the peak values of $|A|$, $|\hat{A}|$, and P_2 increase slightly, showing vibrations with larger amplitude in the substrate and stronger acoustic wave generation.

Fig. 5 presents a global view of the effects of K_0 on the admittance $|A|$, the amplitude $|\hat{A}|$, the energy flux P_2, and the efficiency η when $K_1 = 0.1K_0$. Cases 1 and 2 in the

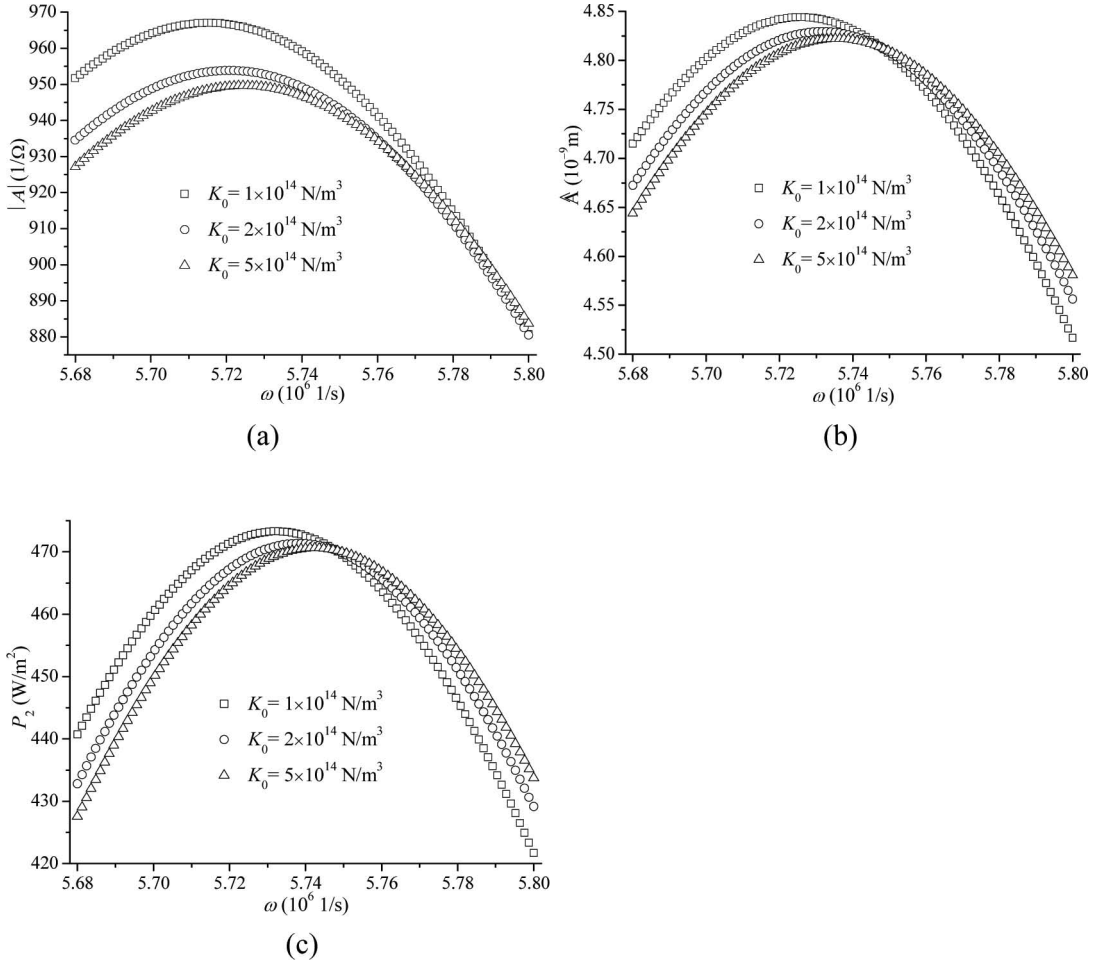

Fig. 4. (a) Admittance $|A|$, (b) amplitude $|\hat{A}|$ of the generated wave, and (c) energy flux P_2 of the generated wave near the first resonance for different K_0 ($K_1 = 2 \times 10^{13}$ N/m^3).

figure are for two different driving frequencies. In Case 1, the driving frequency follows the first resonant frequency as K_0 changes. In Case 2, the driving frequency is fixed to be the first resonant frequency when $K_0 = 1 \times 10^{14}$ N/m^3, which is $\omega = 5.725156 \times 10^6$ 1/s. The figure shows that for large K_0, the corresponding $|A|$, $|\hat{A}|$, P_2, and η approach their limit values when the interface is perfectly bonded. When K_0 is smaller or when the interface becomes weaker, $|A|$, $|\hat{A}|$, and P_2 all increase, but the efficiency η drops monotonically. For $|A|$, $|\hat{A}|$, and P_2, there exist maxima at the same value of K_0. At this K_0, the efficiency is slightly less than its maximum for large K_0 or a perfectly bonded interface. Therefore, this particular value of K_0 at which $|A|$, $|\hat{A}|$, and P_2 assume maxima with a reasonably high efficiency may be viewed as the optimal interface, which is not a perfectly bonded interface. Hence, a weak interface is not necessarily unfavorable and should be considered in the overall design of the transduction structure for optimal performance.

The interface is viscoelastic, as described by a complex K. Table I shows the effect of the interface damping represented by K_1, i.e., the imaginary part of K. From the

TABLE I. Effect of Interface Damping Described by K_1.

K_0 (N/m^3)	K_1/K_0	ω (10^6 1/s)	$\lvert\hat{A}\rvert$ (10^{-9} m)	$\lvert A\rvert$ (1/Ω)	P_2 (W/m^2)	η
1×10^{14}	0	5.724721	4.846585	953.46	473.04	1.0
	0.01	5.724754	4.846534	954.12	473.03	0.9993
	0.1	5.725165	4.845740	959.82	472.95	0.9931
2×10^{14}	0	5.731473	4.829666	949.15	470.85	1.0
	0.01	5.731485	4.829653	949.47	470.85	0.9996
	0.1	5.731653	4.829415	952.37	470.83	0.9965
5×10^{14}	0	5.735595	4.822336	947.66	470.10	1.0
	0.01	5.735598	4.822333	947.80	470.10	0.9999
	0.1	5.735656	4.822270	948.96	470.09	0.9986

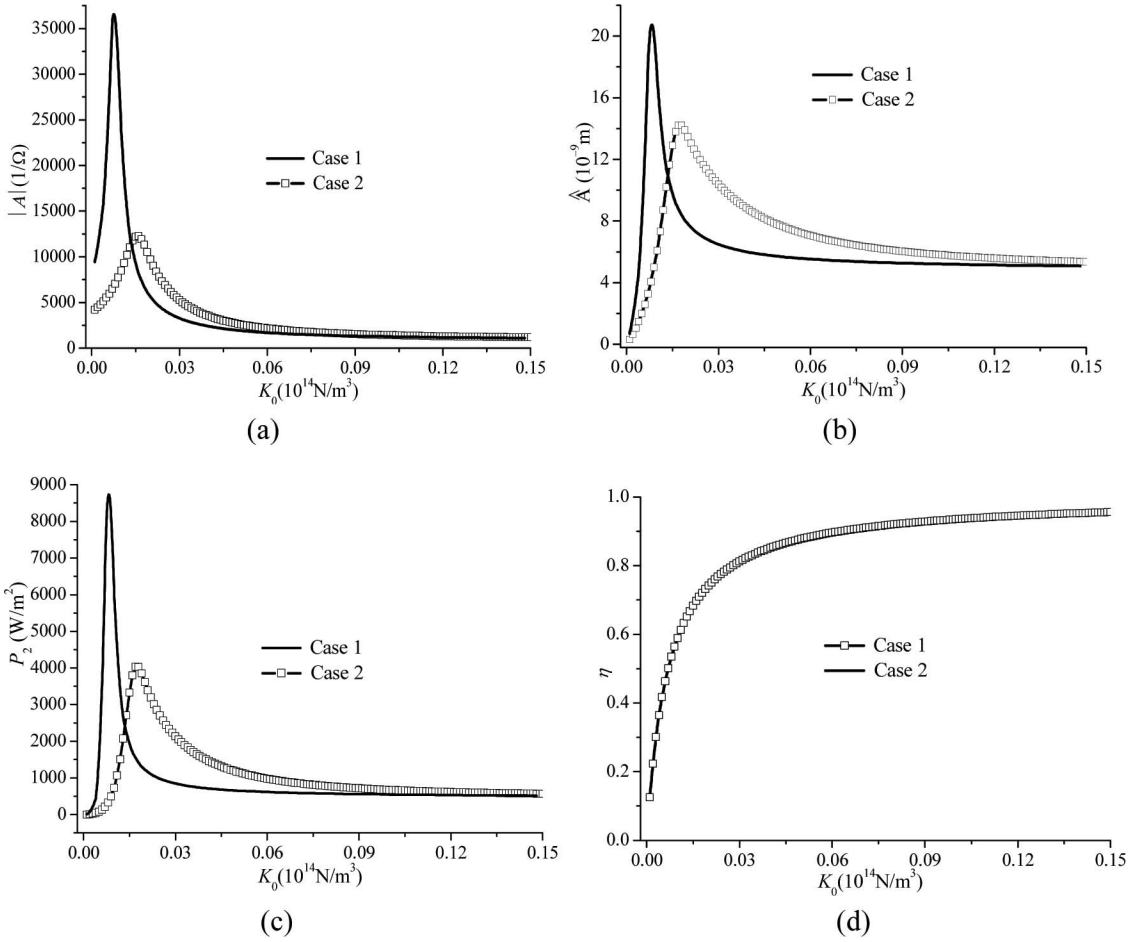

Fig. 5. (a) Admittance $|A|$, (b) amplitude $|\hat{A}|$ of the generated wave, and (c) energy flux P_2 of the generated wave, and (d) efficiency η versus K_0 ($K_1 = 0.1K_0$).

table, it is seen that overall, the effect of K_1 is small. This is because the acoustic wave generated carries the major part of the energy flow which serves as the radiation damping of the transducer and dominates the interface damping.

V. Conclusion

The shear-slip interface model used leads to a jump discontinuity of the tangential displacement at the interface. The interface bonding as part of the stiffness of the whole structure affects the overall transducer performance including the resonant frequency, the amplitude, and energy flux of the acoustic wave generated, the admittance of the structure, and the efficiency of electric–acoustic energy conversion. When the interface bonding is imperfect, although the efficiency drops monotonically, the amplitude and energy flux of the acoustic wave generated, as well as the admittance of the structure, may increase and assume maxima for a particular value of the interface stiffness. The interface damping is a relatively small effect compared with the radiation damping of the acoustic wave generated. Interface analysis should be part of the transduction design for optimal performance. Although the analysis is for shear waves, with a different interpretation of the notation, the analysis is also valid for longitudinal waves generated by a ceramic layer with thickness poling and an interface that is elastic in the normal direction. Therefore, similar behaviors are expected for longitudinal wave generation by piezoelectric transducers.

References

[1] N. M. Newmark, C. P. Ceiss, and I. M. Viest, "Test and analysis of composite beams with incomplete interaction," *Proc. Soc. Exp. Stress Anal*, vol. 91, no. 1, pp. 75–92, 1951.

[2] T.-T. Wu and Y.-C. Chen, "Dispersion of laser generated surface waves in an epoxy-bonded layered medium," *Ultrasonics*, vol. 34, no. 8, pp. 793–799, 1996.

[3] A. I. Lavrentyev and S. I. Rokhlin, "Ultrasonic spectroscopy of imperfect contact interfaces between a layer and two solids," *J. Acoust. Soc. Am.*, vol. 103, no. 2, pp. 657–664, 1998.

[4] F. Jin, K. Kishimoto, H. Inoue, and T. Tateno, "Experimental investigation on the interface properties evaluation in piezoelectric layered structures by Love waves propagation," *Key Eng. Mater.*, vol. 297–300, pt. 1–4, pp. 807–812, 2005.

[5] P. B. Nagy, "Ultrasonic classification of imperfect interfaces," *J. Nondest. Eval.*, vol. 11, no. 3–4, pp. 127–139, 1992.

[6] Z.-Q. Cheng, A. K. Jemah, and F. W. Williams, "Theory for multilayered anisotropic plates with weakened interfaces," *J. Appl. Mech*, vol. 63, no. 4, pp. 1019–1026, 1996.
[7] W. Q. Chen, J. B. Cai, G. R. Ye, and Y. F. Wang, "Exact three-dimensional solutions of laminated orthotropic piezoelectric rectangular plates featuring interlaminar bonding imperfections modeled by a general spring layer," *Int. J. Solids Struct.*, vol. 41, no. 18–19, pp. 5247–5263, 2004.
[8] U. A. Handge, "Analysis of a shear-lag model with nonlinear elastic stress transfer for sequential cracking of polymer coatings," *J. Mater. Sci.*, vol. 37, no. 22, pp. 4775–4782, 2002.
[9] J. P. Jones and J. S. Wittier, "Waves at a flexibly bonded interface," *J. Appl. Mech.*, vol. 34, no. 4, pp. 905–909, 1964.
[10] G. S. Murtya, "A theoretical model for the attenuation and dispersion of Stoneley waves at the loosely bonded interface of elastic half space," *Phys. Earth Planet. Inter.*, vol. 11, no. 1, pp. 65–79, 1975.
[11] S. Leungvichcharoen and A. C. Wijeyewickrema, "Dispersion effects of extensional waves in pre-stressed imperfectly bonded incompressible elastic layered composite," *Wave Motion*, vol. 38, no. 4, pp. 311–325, 2003.
[12] M. X. Deng, P. Wang, and X. F. Lv, "Study of second-harmonic generation of Lamb waves propagating in layered planar structures with weak interface," in *Proc. IEEE Ultrasonics Symp.*, 2006, pp. 1832–1835.
[13] H. Fan, J. S. Yang, and L. M. Xu, "Piezoelectric waves near an imperfectly bonded interface between two half-spaces," *Appl. Phys. Lett.*, vol. 88, no. 20, art. no. 203509, 2006.
[14] H. Fan, J. S. Yang, and L. M. Xu, "Antiplane piezoelectric surface waves over a ceramic half-space with an imperfectly bonded layer," *IEEE Trans. Ultrason. Ferroelectr. Freq. Control*, vol. 53, no. 9, pp. 1695–1698, 2006.
[15] Y. Z. Bai, Y. S. Wang, and G. L. Yu, "Propagation of slip pulse along frictionless contact interface with local separation between two piezoelectric solids," *Appl. Math. Mech.*, vol. 28, no. 9, pp. 1227–1234, 2007.
[16] Y. Z. Bai, Y. S. Wang, and G. L. Yu, "Subsonic slip waves along the interface between two piezoelectric solids in sliding contact with local separation," *Int. J. Eng. Sci.*, vol. 45, no. 12, pp. 1017–1029, 2007.
[17] A. Melkumyan and Y.-W. Mai, "Influence of imperfect bonding on interface waves guided by piezoelectric/piezomagnetic composites," *Philos. Mag.*, vol. 88, no. 23, pp. 2965–2977, 2008.
[18] Y.-D. Li and K. Y. Lee, "Effect of an imperfect interface on the SH wave propagating in a cylindrical piezoelectric sensor," *Ultrasonics*, vol. 50, no. 4–5, pp. 473–478, 2010.
[19] Y. Pang and J. X. Liu, "Reflection and transmission of plane waves at an imperfectly bonded interface between piezoelectric and piezomagnetic media," *Eur. J. Mech. A, Solids*, vol. 30, no. 5, pp. 731–740, 2011.
[20] Y. Y. Chen, J. K. Du, J. Wang, and J. S. Yang, "Shear-horizontal waves in a rotated Y-cut quartz plate with an imperfectly bonded mass layer," *IEEE Trans. Ultrason. Ferroelectr. Freq. Control*, vol. 58, no. 3, pp. 616–622, 2011.
[21] J. A. Otero, R. Rodríguez-Ramos, J. Bravo-Castillero, and G. Monsivais, "Interfacial waves between two piezoelectric half-spaces with electro-mechanical imperfect interface," *Philos. Mag. Lett.*, vol. 92, no. 10, pp. 534–540, 2012.
[22] J. R. Vig and A. Ballato, "Comments about the effects of nonuniform mass loading on a quartz crystal microbalance," *IEEE Trans. Ultrason. Ferroelectr. Freq. Control*, vol. 45, no. 5, pp. 1123–1124, 1998.
[23] F. Ferrante and A. L. Kipling, "Molecular slip at the solid-liquid interface of an acoustic-wave sensor," *J. Appl. Phys.*, vol. 76, no. 6, pp. 3448–3462, 1994.
[24] J. S. Yang, Y. T. Hu, Y. Zeng, and H. Fan, "Thickness-shear vibration of rotated Y-cut quartz plates with imperfectly bonded surface mass layers," *IEEE Trans. Ultrason. Ferroelectr. Freq. Control*, vol. 53, no. 1, pp. 241–245, 2006.
[25] J. K. Chen, W. C. Wang, J. Wang, Z. T. Yang, and J. S. Yang, "A thickness mode acoustic wave sensor for measuring interface stiffness between two elastic materials," *IEEE Trans. Ultrason. Ferroelectr. Freq. Control*, vol. 55, no. 8, pp. 1678–1681, 2008.
[26] J. Zhu, J. S. Yang, and W. Q. Chen, "Locating a weakened interface in a laminated elastic plate," *Struct. Eng. Mech.*, vol. 41, no. 6, pp. 751–758, 2012.
[27] Y. S. Wang, G. L. Yu, Z. M. Zhang, and Y. D. Feng, "Review on elastic waves propagation under complex interface (interface layer) conditions," *Adv. Mech.*, vol. 30, no. 3, pp. 378–389, 2000 (in Chinese).
[28] J. L. Bleustein, "A new surface wave in piezoelectric materials," *Appl. Phys. Lett.*, vol. 13, no. 12, pp. 412–413, 1968.
[29] J. L. Bleustein, "Some simple modes of wave propagation in an infinite piezoelectric plate," *J. Acoust. Soc. Am.*, vol. 45, no. 3, pp. 614–620, 1969.
[30] J. S. Yang, *Antiplane Motions of Piezoceramics and Acoustic Wave Devices*. Singapore: World Scientific, 2010.
[31] Z. H. Qian, F. Jin, Z. K. Wang, and K. Kishimoto, "Dispersion relations for SH-wave propagation in periodic piezoelectric composite layered structures," *Int. J. Eng. Sci.*, vol. 42, no. 7, pp. 673–689, 2004.

Authors' photographs and biographies were unavailable at time of publication.